Histochem Cell Biol (2009) 131:43–53
DOI 10.1007/s00418-008-0515-7

ORIGINAL PAPER

An age-dependent proliferation is involved in the postnatal development of interstitial cells of Cajal in the small intestine of mice

Feng Mei · Jiang Zhu · Sheng Guo · De-shan Zhou · Juan Han · Bin Yu · Shi-feng Li · Zhong-yong Jiang · Cheng-jie Xiong

Accepted: 13 September 2008 / Published online: 3 October 2008
© Springer-Verlag 2008

Abstract This paper aimed at investigating the alterations in interstitial cells of Cajal (ICCs) in the murine small intestine from 0-day to 56-day post-partum (P0–P56) by immunohistochemistry. The Kit$^+$ ICCs, which were situated around myenteric nerve plexus (ICC-MY) formed a loose cellular network at P0 which changed into an intact one before P32. The density of ICC-MY increased from P0 to P12, and then decreased until P32. In contrast, the estimated total amount increased more than 15-fold at P32 than that at P0. Some Kit$^+$/BrdU$^+$ cells were observed at 24 h after one BrdU injection to the different-aged mice, and the number decreased from P2 to P24 and vanished at P32. Actually a few Kit$^+$/BrdU$^+$ cells can be observed at 1 h after one BrdU injection at P10, and the amount doubled at 24 h along with paired Kit$^+$/BrdU$^+$ cells. A number of BrdU$^+$ ICCs were also labeled with CD34, CD44 and insulin-like growth factor I receptor. About 65% ICCs were BrdU$^+$ at P32 after daily BrdU injection from P0. Our results indicate that an age-dependent proliferation is involved in the postnatal development of ICC-MY which increase greatly in cell numbers and proliferative ICCs may originate from ICCs progenitor cells.

Keywords Proliferation · Kit · BrdU · Precursor · Progenitor

Feng Mei and Jiang Zhu have contributed equally to this work.

Electronic supplementary material The online version of this article (doi:10.1007/s00418-008-0515-7) contains supplementary material, which is available to authorized users.

F. Mei (✉) · D.-s. Zhou · J. Han · B. Yu · S.-f. Li · Z.-y. Jiang · C.-j. Xiong
Department of Histology and Embryology,
Third Military Medical University, 400038 Chongqing, China
e-mail: thethirdmilitary@sohu.com

J. Zhu
Department of Pathology, Southwest Hospital,
Third Military Medical University, 400038 Chongqing, China

S. Guo
Department of Immunology, Third Military Medical University,
400038 Chongqing, China

D.-s. Zhou
Department of Histology and Embryology,
Capital University of Medical Sciences, 100054 Beijing, China

Introduction

Maturation related alterations in intestinal structure are important for the development of small intestinal motility throughout the postnatal period (Thomson and Keelan 1986). The diameter, length and wall-thickness of the small intestine of adult animals have increased several folds when compared with measurements obtained from neonates. In addition, intestinal contractions and motility are greatly enhanced after birth (Lu et al. 2005).

It is widely accepted that interstitial cells of Cajal (ICCs) play an important role in the regulation of gastrointestinal motility (Thomsen et al. 1998). ICCs express *c-kit* gene product, Kit (a tyrosine kinase receptor) (Huizinga et al. 1995), which is essential for the determination of cell lineage, survival and proliferation during embryonic and neonatal periods (Torihashi et al. 1999; Beckett et al. 2007), and is a marker protein of ICCs. Kit positive ICCs or their precursors of ICCs first appear in the murine intestinal wall at E12.5 (Torihashi et al. 1997; Young et al. 1996) and subsequently, start to cluster around the myenteric nerve plexus. At the time of birth, one layer of ICCs, so called

ICC-MY, is located between the longitudinal and circular smooth muscle layers (Ward and Sanders 2001). Studies have shown that ICC-MY fully differentiate and mature 48 h after birth and possess identical ultrastucture and electrophysiological activity (Liu et al. 1998). These cells act as the pacemaker cells that generate and propagate the slow waves (Lee et al. 1999; Ordog et al. 1999). ICC-DMP, another subtype of ICC in the small bowel, which are closely associated with nerve fibers (Ward et al. 2006; Zhou and Komuro 1992), and appear soon after birth (Ward and Sanders 2001). However, the postnatal development of ICCs, from neonatal to adult life, is poorly investigated, although the small intestine keeps lengthening and extending throughout this period, in spite of the fact that developmental disorders related to ICCs have been shown to be involved in a number of dysfunctions of the gastrointestinal tract in newborns and infants, such as intestinal pseudo-obstruction (Krishnamurthy et al. 1993), Hirschsprung's disease (Vanderwinden et al. 1996b) and infantile hypertrophic pyloric stenosis (Vanderwinden et al. 1996a).

Moreover, the progenitor of ICCs in the postnatal gastrointestinal tract has, until now, not yet been unambiguously identified. A recent research has identified a type of cell, rare and resembling ICCs progenitor, which can be expanded by soluble Kit ligand, stem cell factor (SCF), and further differentiate into mature ICCs (Lorincz et al. 2008). Similarly, several in vitro experiments have shown that SCF can expand ICCs obtained from the embryonic and neonatal murine intestine (Wu et al. 2000), however, ICCs from the mice older than day-6 post-partum do not proliferate (Nakahara et al. 2002) and suggests that the proliferation of ICCs is time-limited and SCF-dependent under the culture conditions. In spite of the clear evidence for proliferation in vitro, it is not clear yet whether the proliferation of ICCs is involved in the postnatal development of ICCs.

To answer this question, we have used immunofluorescent staining to study alterations in morphology and number of ICCs in the murine small intestine over the period extending from neonatal (P0) to adult (P56) life.

Materials and methods

Animals

BALB/C mice were purchased from the Animal Center of the Third Military Medical University (Chongqing, China) and paired to produce offspring. Eighty-seven postnatal mice were used in our experiments. Animals were divided into 4 groups: 1) Twenty-four mice were killed at postnatal day 0 (P0), P2, P5, P8, P16, P24, P32 and P56; 2) twenty-one mice were injected with one dose of BrdU (0.1 mg/g) intraperitoneally 24 h before sacrifice at P2, P5, P8, P16, P24, P32 and P56; 3) twenty-one mice were injected daily with BrdU from P0 and were killed at P2, P5, P8, P16, P24, P32 and P56; 4) twenty-one mice were given one injection of BrdU (0.1 mg/g) on P10 and were killed at 1, 2, 8, 16, 24, 48 and 96 h later. All experiments were performed in accordance with our University Health Guide for the Care and Use of Laboratory Animals.

Immunofluorescence

Ten to five minutes before the abdomen was opened to expose the small intestine, a dose of papaverine (0.12 mg/g), a calcium antagonist, was injected intraperitoneally in order to abolish contractile activity in the small intestine. The entire small intestine from the pylorus to ileo-caecal junction was removed tenderly and placed into the PBS containing papaverine (0.5 mg/ml), and then the length and diameter of the small intestine were measured quickly. To obtain whole-mount preparations, the small intestine was inflated with acetone to the size identical with the one when the parameters were measured formerly. After 30 min fixation, and the longitudinal smooth muscle layer containing the ICC-MY was prepared with the aid of a dissection microscope. The immunostaining procedures have been previously described (Komuro and Zhou 1996). Briefly, after the specimens were incubated with primary antibody (Table 1) for 8 h at 4°C, the immunoreactivity was detected by using a Cy3-conjugated secondary antibody (anti-rat IgG, 1:100; Zymed), or FITC-conjugated secondary antibody (anti-mouse IgG, 1:100; DAKO), or Cy5-conjugated secondary antibody (anti-rabbit IgG, 1:100; Zymed). To identify the proliferation of ICCs, the whole-mount preparations were stained for ACK2 (Kit) as described above, and then double labeled for BrdU as follows: the specimens were additionally fixed in 4% paraformaldehyde in 0.1 M PB at pH 7.2 for 10 min. After rinsing in PBS, the specimens were treated with 2N HCl for 30 min at 37°C. To reveal BrdU labeling, the specimens were incubated with a mouse monoclonal antibody raised against BrdU (3 μg ml^{-1}; DAKO) overnight at 4°C and then incubated with a FITC-conjugated secondary antibody (anti-mouse

Table 1 The primary antibodies

Antigen	Clone	Supplier	Dilution	Isotype
Kit	ACk2	eBioscience	1:100	Rat IgG
BrdU	Bu20a	DAKO	1:100	Mouse IgG
Vimentin	V9	Neomarker	1:200	Mouse IgG
IGF-1	Polyclone	Santa Cruz	1:100	Rabbit lgG
IGF-1R	Polyclone	Neomarker	1:100	Rabbit lgG
CD34	Polyclone	Boster	1:100	Rabbit lgG
CD44	Polyclone	Boster	1:100	Rabbit lgG

IgG, 1:100; DAKO). The stained results were examined with a BX51 fluorescence microscope (OLYMPUS, Japan) or a TCS SP5 confocal laser scanning microscope (Leica, Germany) with an excitation wavelength appropriate for Cy3 (552 nm), FITC (488 nm) and Cy5(625 nm). The Z stacking of confocal images at 3–5 μm intervals contained all the levels of positively stained cells and processes.

Measurement and statistical analysis

Six intestinal segments from each experimental animal were sampled in a random manner and intestinal diameter measured and immunofluorescent staining assessed. Photomicrographs of both Kit positive cells and Kit/BrdU double labeled cells were taken in 10 random fields (×200 magnification, 0.2607 mm^2) per whole-mount preparation with a digital camera (SPOT, Diagnostic Instruments, Inc) mounted on a BX51 fluorescence microscope (OLYMPUS, Japan). The numbers of either Kit positive cells or Kit/BrdU double labeled cells were counted with Image-Pro Plus 5.0 (Media Cybernetics). The estimated surface area of ICC-MY in the small intestinal wall = (mean diameter − 2 × mean thickness of longitudinal smooth muscle layer) × π × length. Multiplying the estimated surface area of ICC-MY and mean density together made the estimated total cell number of ICC-MY. Data are expressed as means ± S.E.M. The n value reported in the text refers to the number of animal used. Differences in the data were evaluated by student t test, and $P < 0.05$ was taken as a statistically significant difference.

Results

Morphologic alterations of ICCs

The Kit positive ICC-MY were observed between the longitudinal and circular muscular layers around the myenteric nerve plexus. In the duodenum and jejunum at birth (P0)(Group 1), these cells were arranged into a loose cellular network that connected with each other via 2–3 short and slim processes with several branches (Fig. 1a, b). In comparison, ICC-MY in the ileum seemed to have fewer and shorter processes, or lacked definitive processes entirely, thus making the network seem incomplete (Fig. 1c). By P2 and P5, the processes of ICC-MY in the duodenum and jejunum were more numerous and longer but had thinner processes with branches than compared with that seen at P0 (Fig. 1d, e). Similar changes were seen in the ileum, albeit the processes were shorter and lower in number (Fig. 1f). Subsequently, at P8 and P12, the Kit-postive cells increased in density and possessed thicker and more abundant processes, and an compact cellular network was seen (Fig 1g–i). These cells were similar to the morphologically mature cells observed in P16 animals, which had a large number of winding branching processes. Well-developed ICCs cellular networks were observed in duodenum, jejunum and ileum by P32 (Fig. 1j–l) and P56.

Density and estimated total cell number of of ICCs

The quantitative data showed that the mean density of Kit-positive ICC-MY in the small intestine was about ~750 mm^{-2} at P0, increasing to a maximum of 1,010 mm^{-2} at P12 (Table 2). Subsequently, the cell number decreased to about 720 mm^{-2} at P32, a value which was similar to that seen in adult mice (P56) (Table 2). The length and the average diameter of small intesine were 71.3 and 0.98 mm respectively at P0, and these values increased to 297.2 and 3.93 mm by P32 (Table 2). The estimated area of the small intestinal wall increased about 17-fold from 200 mm^2 at P0 to 3,520 mm^2 at P32 (Table 2). Therefore, given the density of ICC-MY and the estimated area of small intestinal wall, the total cell number of ICC-MY was estimated at about 1.52×10^5 at P0 and at 25.29×10^5 at P32, suggesting a more than 15-fold increase in total cell number (Table 2).

Detection of proliferative ICCs

In the preceding section we showed that the total number of ICC-MY increased by more than 15-fold. We wished to know the underlying mechanisms for this increase and therefore BrdU was used to detect the presence of proliferative events of ICCs. BrdU was incorporated into Kit positive cells 1–2 h after injection into the P10 mice (Group 4), most cells had 2–3 thick processes without branch and were not connected with the cellular network (Fig. 2a–c), The number of such cells amounted to 32.4 and 48.2 mm^{-2} at 1 and 2 h respectively (Table 3). Then paired Kit/BrdU double labeled cells began to show up 8 h post-BrdU-injection, and the double positive cells always distributed in pairs at 24 h (Table 3). Each paired double labeled cells was characterized by closely located cell bodies and similar features (Fig. 2d–f). Quantitation showed that the cell numbers had nearly doubled within 24 h (Table 3). These cells further developed into the cells with prolonged processes and branches and had features similar to those of mature ICC-MY 48 h later (Fig. 2g–i), although the density decreased slightly at 48 and 96 h, possibly due to the expansion intestinal wall area (Table 3).

Proliferative ability of ICCs

To investigate the proliferative ability of mice with different ages, BrdU/Kit double labeled ICC-like cells were detected 24 h after one dose of BrdU injection (Group 2).

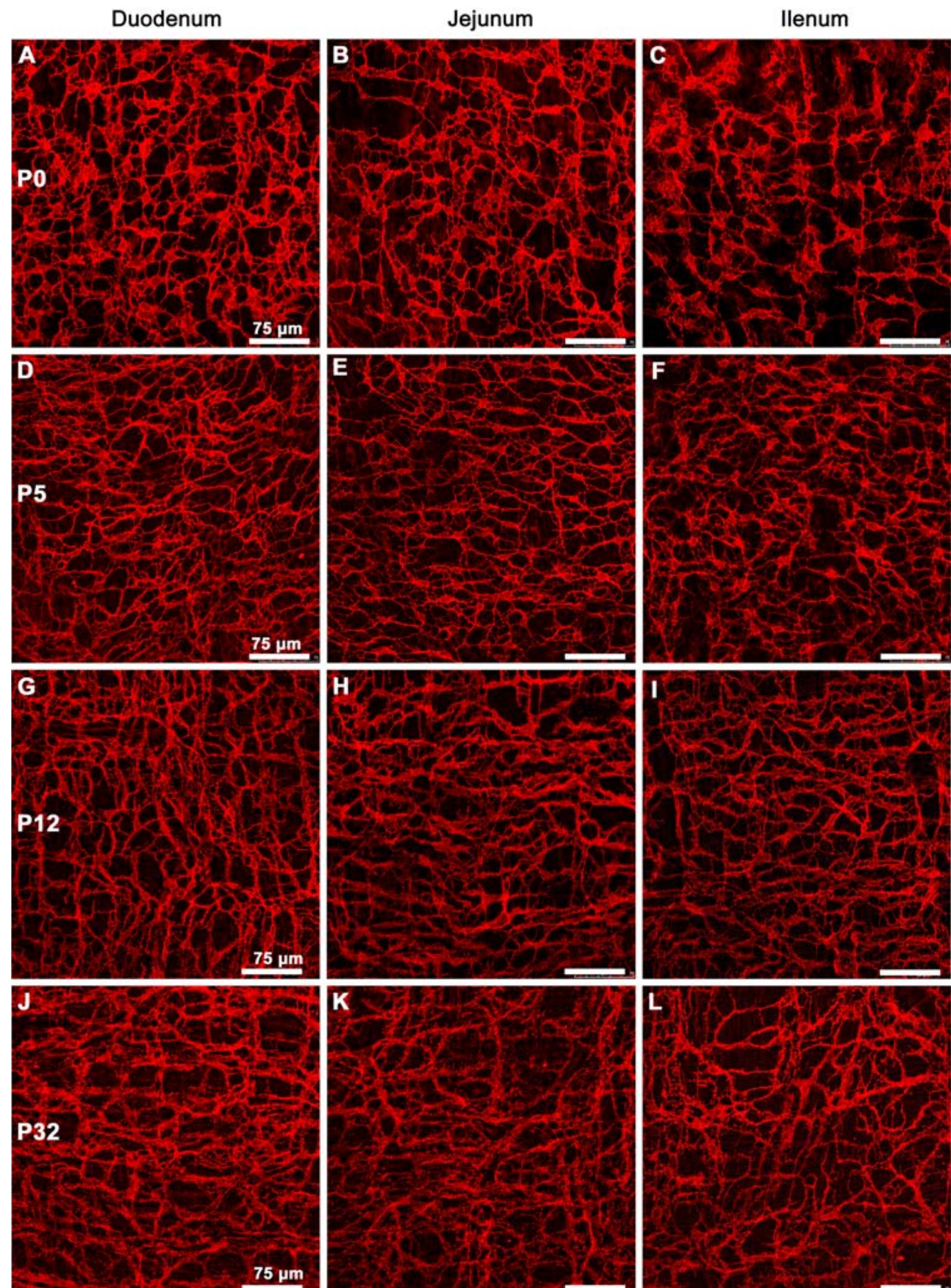

Fig. 1 Confocal images of murine small intestine whole-mount preparations. ICC-MY were labeled with Kit and illustrate alterations of ICC morphology and density in the duodenum (**a**, **d**, **g**, **J**), jejunum (**b**, **e**, **h**, **k**), and ileum (**c**, **f**, **i**, **l**) at P0 (**a–c**), P5 (**d–f**), P12 (**g–i**) and P32 (**j–l**). **a–c:** ICCs formed a loose cellular network interconnected by 2–3 slim, short, primary processes with very few branch at P0; ICCs in the duodenum (**a**) and jejunum (**b**) seemed to be better developed compared with cells in the ileum (**c**). **d–f**: ICCs had more elongated and slim processes with several branches and had a higher density at P5 in the duodenum (**d**) and jejunum (**e**), while ICCs of the ileum had comparably fewer processes and a lower density (**f**). **g–i** At P12, ICCs projected their thick cytoplasmic processes to form an intact cellular network, which was not so apparent in the ileum (**i**). **j–l**: ICCs developed further into a complicated network with gross processes at P32, which were almost identical to that of adult. *Scale bar* **a–l** 75 µm

The analysis showed that the BrdU labeled ICCs were seen frequently on whole mount preparations (Fig. 3a–c), and about 178.4 such cells (mm^{-2}) were observed at P2 (Table 4). The value gradually decreased to 102.2 and 68.4 respectively by P8 (Fig. 3d–f) and P16 (Fig. 3g–i) (Table 4). The BrdU positive ICC-MY were rare in P24 samples (Fig. 3j–l) and were not present by P32 (Fig. 3m–o) or P56 (Table 4). These results suggest that ICC proliferation is age-dependent and may cease just beyond P24.

To determine the fraction of ICC-MY which resulted from proliferation, daily BrdU injection was performed from birth until the animals were killed (Group 3). At P2, about 28% ICC-MY were both Kit and BrdU positive. The fraction increased to 35% at P5 (Fig. 4a–c; Table 4), reaching a peak value of 64% by P24 (Fig. 4d–f) and P32 (Table 4), which implied that ICC-MY expanded their volume mainly by the way of proliferation.

Origin of the proliferative ICCs

Since vivid proliferation was seen in the postnatal development of ICCs, then we wanted to investigate the origin of these proliferating ICCs. A recent study has identified a very small group of $Kit^{+}/CD44^{+}/CD34^{+}$/insulin $receptor^{+}$/

Table 2 The mean density and estimated total cell number of Kit positive ICC-MY, and the mean diameter, full length and estimated total area of the small intestinal wall of mice with different ages from P0 to P56

	P0	P2	P5	P8	P12	P16	P24	P32	P56
Mean density of Kit$^+$ ICC-MY in small bowel (mm^{-2}) ($N = 3$)	749.2 ± 20.3	841.5 ± 21.9*	903.5 ± 11.2*	951.6 ± 20.0*	1010.1 ± 21.1*	966.9 ± 15.7*	786.7 ± 28.1*	725.3 ± 20.2*	716.9 ± 29.2
Estimated total amounts of ICC-MY ($\times 10^5$) ($N = 3$)	1.52 ± 0.09	2.74 ± 0.08*	4.81 ± 0.05*	8.14 ± 0.13*	11.61 ± 0.21*	14.10 ± 0.19*	22.07 ± 0.30*	25.29 ± 0.37*	25.27 ± 0.24
Mean diameter of small intestine (mm) ($N = 3$)	0.98 ± 0.10	1.22 ± 0.11*	1.59 ± 0.16*	2.12 ± 0.20*	2.49 ± 0.10*	2.76 ± 0.11*	3.71 ± 0.34*	3.93 ± 0.27	3.98 ± 0.23
Full length of small inestine ($\times 10$ mm) ($N = 3$)	7.13 ± 0.32	9.23 ± 1.24*	11.01 ± 0.86	13.54 ± 1.01*	15.58 ± 1.82	17.45 ± 3.32	25.58 ± 2.12*	29.72 ± 3.19	30.81 ± 2.42
Estimated total area ($\times 10^3$ mm^2) ($N = 3$)	0.20 ± 0.03	0.33 ± 0.04*	0.53 ± 0.04*	0.86 ± 0.06*	1.15 ± 0.09*	1.46 ± 0.10*	2.80 ± 0.18*	3.49 ± 0.21*	3.52 ± 0.33

Data given as mean ± S.E.M

N numbers of mice used

*Significantly different to the earlier time-point (i.g., P5 vs P2) ($P < 0.05$)

insulin-like growth factor I receptor (IGF-IR)$^+$ cells in murine stomach as the putative progenitors of ICCs (Lorincz et al. 2008). Interestingly, our results showed that most Kit/BrdU double positive cells were also labeled with CD44 (*arrows* Fig. 5a–d) and a number of Kit$^+$/BrdU$^+$ cells were also labeled with IGF-IR (*arrow* Fig. 5e–h) in the mice after one dose BrdU injection for 1 h at P10 (Group 4). In addition, CD34, a cellular marker of hematopoeitic cells and endothelial cells of blood vessels, was also found expressed by a number of BrdU labeled ICC-MY (*arrowhead* Fig. 5i–l). Besides that, vimentin$^+$/IGF-I$^+$ fibroblast-like cells are regarded as the progenitors of ICCs (Pucilowska et al. 2000). Our finding indicated that such cells were very rare around myenteric plexus in the small intestine (*arrow* Fig. 5m–o) which suggested these cell might the progenitors of ICCs in a certain situation.

Discussion

The present study demonstrates that: (1) The estimated total cell number of Kit positive ICCs increases about 15-fold from neonatal to adult life in mice along with the extension and elongation of the small intestine; (2) ICCs expand their volume mainly by an age-dependent proliferation which persists from day-0 to day-24 post-partum; (3) Some of the newly emerged Kit/BrdU double positive cells were also labeled with CD34, CD44 and IGF-IR which implies ICCs progenitors may be the origin of proliferation.

Morhphogic and quantitative alterations of ICCs

ICCs begin to appear during the embryonic period (Torihashi et al. 1995; Faussone-Pellegrini et al. 1996; Torihashi et al. 1997; Ward et al. 1997), and the ICC-DMP first appear at the time of birth (Ward and Sanders 2001). ICC-MY are immature at birth both in ultrastructure and physiologic functions (Liu et al. 1998). About 2 days after birth, ICC-MY develop ultrastructural features and electrophysiological features that are essentially identical to mature ones (Faussone-Pellegrini et al. 1996; Liu et al. 1998). Our results show that Kit-positive ICC-MY are loosely interconnected with each other by several slim and very short processes, and a loose cellular network is observed at birth. A complete cellular network is seen at P2, with increasing thick, branching processes appearing from P5 to P32. The processes of ICCs are closely connected with SMCs and enteric nerves which can propagate the slow waves and receive nervous integration (Rumessen and Thuneberg 1991). The gradual enrichment and growth of processes might contribute to the postnatal development of the intestinal motility, in other words these morphological alterations would be adapted for the large increase in smooth muscle

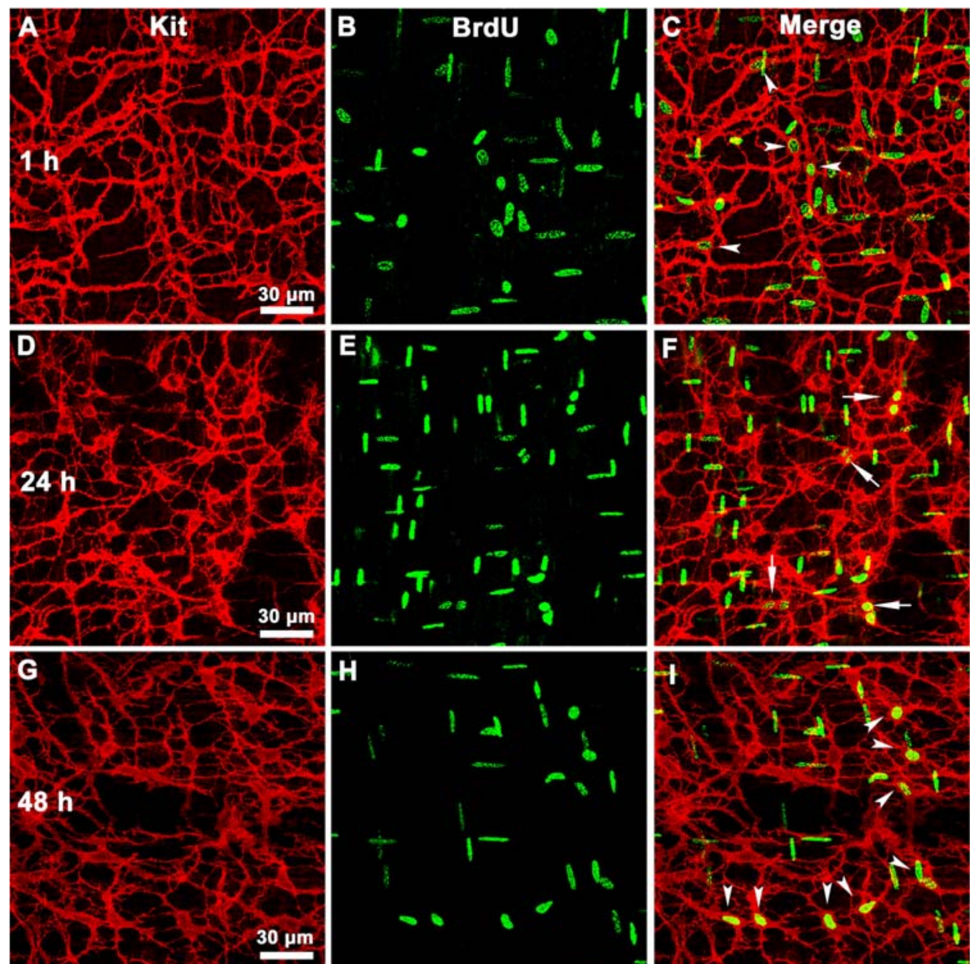

Fig. 2 Confocal microphotographs showing presumptive proliferations of ICCs on whole mount preparations of ileum in the mice at P10. **a–c** A number of double labeled Kit$^+$ (*red*) and BrdU$^+$ (*green*) cells (*arrowheads*) were observed 1 h after one dose of BrdU injection. These cells had 2–3 thick processes without branches, and did not appear mature. **d–f** Kit$^+$/BrdU$^+$ were often distributed in pairs at 24 h, each pair of these cells had adjacent cell bodies (*arrows*) and identical profiles. **g–i** These paired double labeled cells (*arrowheads*) had developed features similar to those of mature cells at 48 h. *Scale bar*: **a–i** 30 μm

Table 3 The density of Kit/BrdU double labeled cells in ICC-MY of the mice10-day post-partum from 1 to 96 h after one dose of BrdU injection

	1 h	2 h	8 h	16 h	24 h	48 h	96 h
The density of Kit$^+$/BrdU$^+$ cells after one dose of BrdU injection (mm^{-2}) ($N = 3$)	32.4 ± 3.3	48.2 ± 3.6*	54.2 ± 5.3	78.5 ± 4.6*	93.4 ± 3.3*	81.6 ± 5.2*	73.4 ± 5.7

Data given as mean ± SEM

N numbers of mice used

*Significantly different to the earlier time-point (i.e., P5 vs. P2) ($P < 0.05$)

cells (Lu et al. 2005) and enteric neurons. In addition, it seems that ICC-MY of the duodenum and jejunum develop sooner and are morphologically better than those of the ileum, which is probably due to a better developed motility in these regions (Lu et al. 2005).

The small intestine increases in diameter and prolongs in length for multi-fold from postnatal period to adulthood in rats (Lu et al. 2005), and our results reveal similar alterations in mice. Accordingly the estimated wall area of small intestine increases more than 17-fold during this period. The mean density of ICC-MY does not alter dramatically with an increase of approx 40% from P0 to P12 and then decreased by approx 30% at P32. However, it is noteworthy that the estimated total number of ICCs in the small intestine increases by more than 15-fold over the neonatal to adulthood period in mice. This result indicates that ICCs would keep increasing in cell number during postnatal development rather than remaining constant.

Proliferation of ICCs

Considering great increase of the ICCs cell number, the question arises what mechanism is involved in the dramatic increase in cell number? BrdU incorporation has been applied to detect the proliferative ICCs. Our result shows that, after daily injection of BrdU from birth, about 28% of

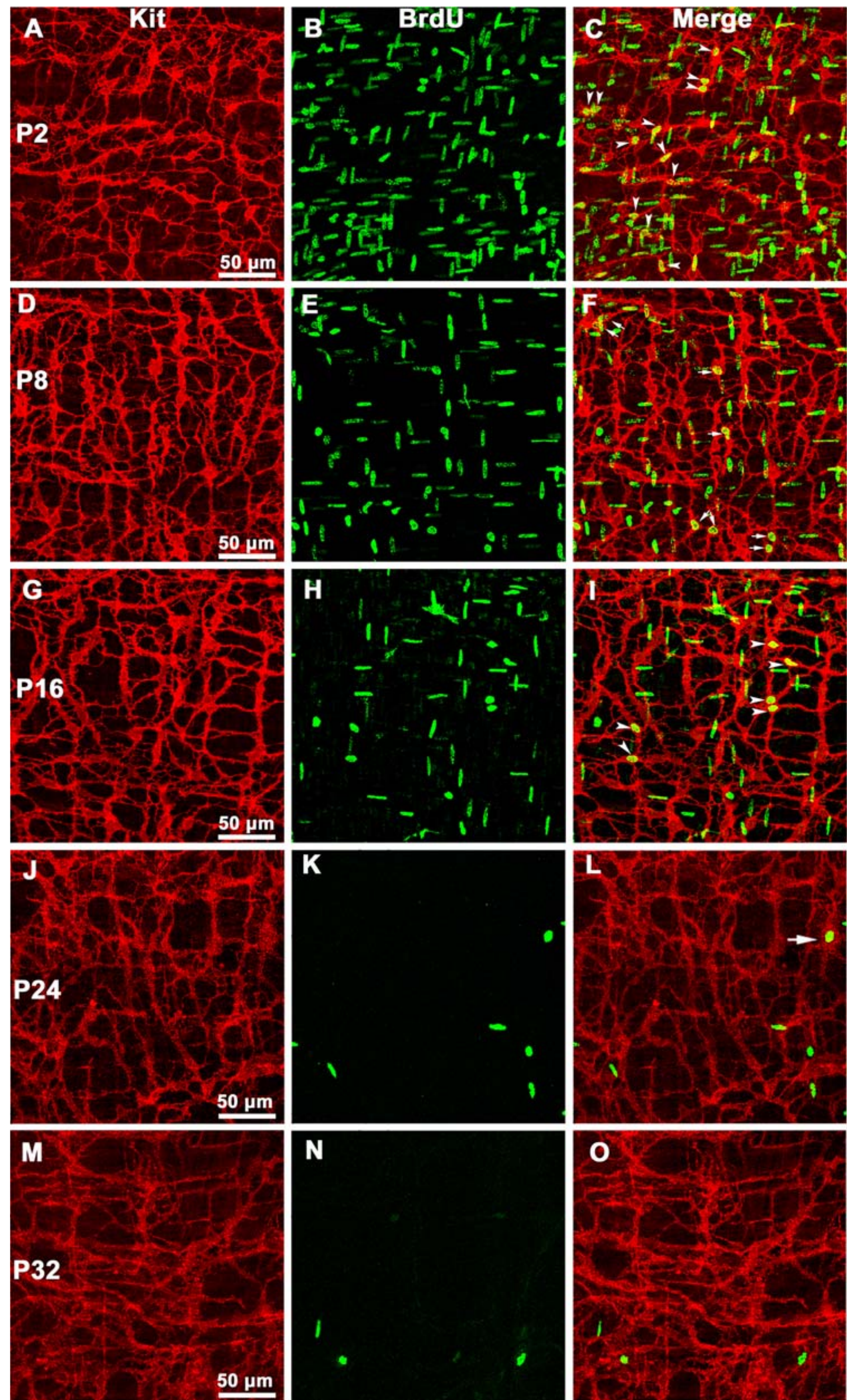

Fig. 3 Confocal images of ICC-MY labeled with Kit (*red*) and BrdU (*green*) on whole-mount preparations of the murine ileum at P2 (**a**–**c**), P8 (**d**–**f**) and P16 (**g**–**i**) showing the proliferation of ICCs 24 h after a single dose of BrdU. **a**–**c** At P2, a large amount of Kit/BrdU double labeled cells (*arrowheads*) were observed with slim and short processes. **d**–**f** At P8, ICC-MY had longer and thicker processes, some of which were both Kit and BrdU positive (*arrows*); the number of these cells was less than that seen at P2. **g**–**i** At P16, a number of $Kit^+/BrdU^+$ (*arrowheads*) also could be observed, which indicated that the proliferation of ICCs persist until early adulthood. The BrdU positive ICC-MY were rare to see (*arrow*) in P24 samples (**j**–**l**) and were not present by P32 (**m**–**o**). *Scale bar*: **a**–**o** 50 µm

Kit labeled ICCs are also BrdU positive at P2, and this ratio increases to 65% by P32, thus indicates the proliferation is a major method for ICCs to expand their volumes. Besides that, to measure the proliferative ability of ICCs of the small intestine at different ages, the incorporation of BrdU is detected at 24 h after one dose injection of BrdU to mice

Table 4 Mean density and percentage of Kit/BrdU double labeled cells in the ICC-MY of the mice with different ages after one dose of BrdU injection for 24 h or daily injection of BrdU from birth

	P2	P5	P8	P12	P16	P24	P32
The density of $Kit^+/BrdU^+$ cells at 24 h after one dose of BrdU injection (mm^{-2}) ($N = 3$)	178.4 ± 22.3 (24%)	123.6 ± 8.6* (15%)	102.2 ± 6.4* (11%)	85.5 ± 7.6* (9%)	68.4 ± 3.3*(7%)	8.1 ± 1.2*(1%)	0*(0%)
The density of $Kit^+/BrdU^+$ cells after daily injection of BrdU from birth (mm^{-2}) ($N = 3$)	235.6 ± 13.5 (28%)	316.2 ± 20.5* (35%)	409.2 ± 40.3* (43%)	551.2 ± 67.1* (51%)	515.2 ± 53.6 (57%)	495.6 ± 40.1 (64%)	471.4 ± 32.9 (65%)

Data given as mean ± SEM No Kit/BrdU double labeled cells was observed at P56

N numbers of mice used

*Significantly different to the earlier time-point (i.g., P5 vs. P2) ($P < 0.05$)

with different ages. It is noteworthy that the BrdU/Kit double labeled ICC-like cells are most abundant on day-2 and are still added until day-24 post-partum albeit in declining numbers, after which ICCs addition ceases. These results strongly suggest that the proliferation of ICCs is age-dependent and can persist from neonatal to almost adult life. In contrast, under in vitro culture conditions, only ICCs obtained from mice before P6 can proliferate in response to Kit ligand which suggests a time-limited and SCF-dependent proliferation of ICCs (Nakahara et al. 2002). The difference between in vitro and in vivo conditions might be explained by the fact that in vivo conditions are more appropriate for proliferation of ICCs than that in vitro conditions, i.e. proliferation of ICCs is dependent on suitable microenvironments. Addition of the Kit blocker (Imatinib) to organ cultures of the small intestine of juvenil mice leads to loss of ICCs, however, ICCs do reappear after removal of the agent (Beckett et al. 2007). Similarly ICCs in the small intestine of adult animals can regenerate after a reduction in cell numbers following gut transection and anastomsis (Yanagida et al. 2004; Mei et al. 2006), or obstruction (Chang et al. 2001). The recovery of ICCs in these cases might be the result of a re-expression of Kit protein of ICCs. Proliferation of ICCs or ICCs precursors is evident in the postnatal development, thus it is probable that proliferative events are also involved in the recovery of ICCs numbers as well as the resumption of Kit receptor.

Origin of the proliferative ICCs

Several investigations have proven that ICCs originate from mesenchymal cells (Kluppel et al. 1998; Lecoin et al. 1996; Wu et al. 2000; Young et al. 1996; Young 1999). The precursors of ICCs have the ability to differentiate towards ICCs under the stimulation of Kit signaling (Ward and Sanders 2001). A recent study has identified a very small group of $Kit^+/CD44^+/CD34^+$/insulin $receptor^+$/insulin-like growth factor I receptor $(IGF\text{-}IR)^+$ cells in murine stomach as the putative progenitors of ICCs which could be expanded under the stimulation of SCF (Lorincz et al. 2008). The present study shows that BrdU is initially only incorporated (within an hour after injection) into a type of Kit positive cell with bi- or tripolar thick processes without branches, which does not seem to be mature ICC-MY. Then paired Kit^+/BrdU labeled cells are often encountered 24 h post-BrdU-injection, concomitant with a cell number doubling. These paired cells further change into the features similar with mature ones. Besides that, some of $Kit^+/BrdU^+$ cells were also labeled with CD44, IGF-IR and CD34. Therefore, it is possible that these Kit positive cells with thick bi- and tripolar might be ICCs precursors at a certain stage of commitment (Huizinga and White 2008; Lorincz et al. 2008) that can proliferate and further differentiate into

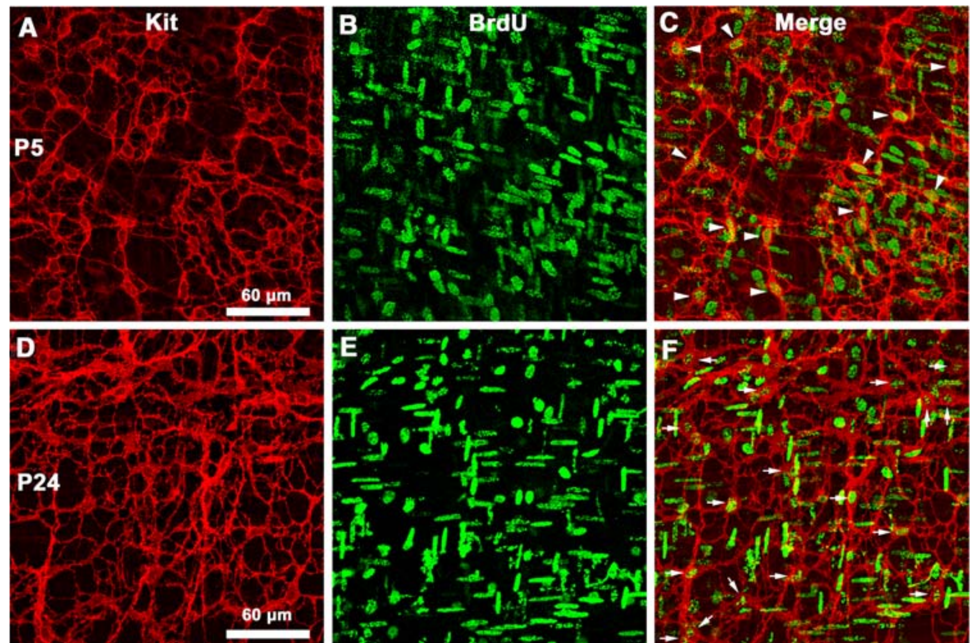

Fig. 4 Confocal microphotographs showing the ICCs which emerged by proliferation on whole mount preparations of ileum with daily injection of BrdU from P0. **a**–**c** A large number of double labeling of Kit (*red*) and BrdU (*green*) cells (*arrowheads*) were observed at P5. More double positive cells (*arrows*) were seen at P24 (**d**–**f**). *Scale bar*: **a**–**f** 60 μm

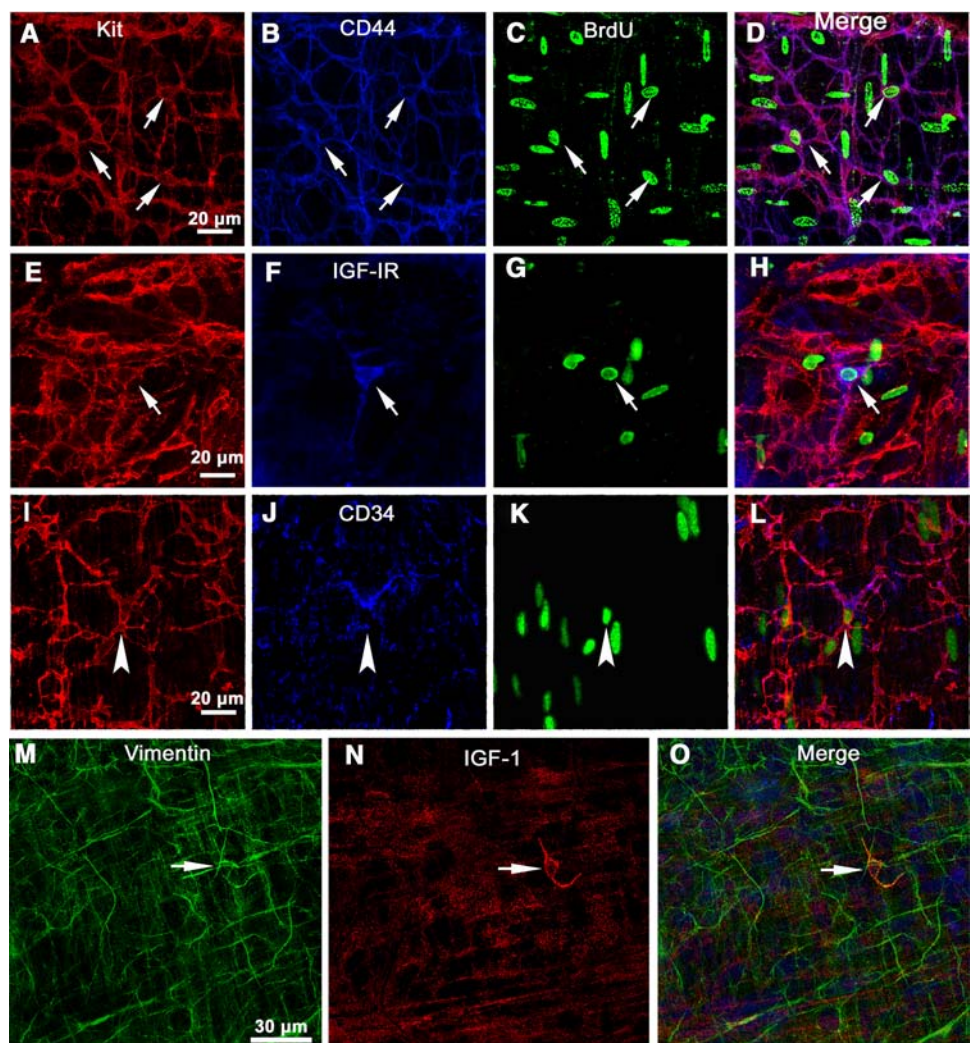

Fig. 5 Confocal microphotographs showing the Kit$^+$/BrdU$^+$ cells expressing CD44 (**a**–**d**), IGF-IR (**e**–**h**) and CD34 (**i**–**l**) on whole mount preparations of small intestine in the mice at P10 after one dose BrdU injection. **a**–**d** Most Kit (*red*)/BrdU (*green*) double labeled cells were also CD44 positive (*blue*) (*arrows*). A number of them were stained with IGF-IR (*blue*) (*arrow*) (**e**–**h**), or CD44 (*blue*) (*arrowhead*) (**i**–**l**). **m**–**o** Very rare vimentin$^+$ (*green*)/IGF-I$^+$ (*red*) fibroblast-like cells were observed on whole mount preparations (*arrow*) counterstained with DAPI (*blue*) at P8. *Scale bar*: **a**–**l** 20 μm, **m**–**o** 30 μm

mature ICCs during the postnatal development. However, further investigations into the ultrastructural, physiologic and biologic characteristics of these cells are necessary to further substantiate this hypothesis.

In addition, vimentin$^+$/IGF-I$^+$ fibroblast-like cells are regarded as the progenitors of ICCs (Pucilowska et al. 2000), and ICC progenitor cells may switch their Kit expression (Horiguchi and Komuro 2000). And it may be possible that the Kit phenotype may switch between mature ICC and fibroblast-like progenitor cells. Our finding indicates that these vimentin$^+$/IGF-I$^+$ fibroblast-like cells are very small in amount (<2%) in the small intestine comparing with the Kit$^+$ cells from P0 to P32 (data not shown) which suggested these cells might the progenitors of ICCs at certain stage and the switch of the phenotype between mature ICCs and the progenitor seemed to contribute slightly to the proliferation of ICCs and increase of ICCs cell numbers.

It is known that a number of motility disorders in children are associated with the reduced ICCs numbers, such as intestinal pseudo-obstruction (IPO) (Isozaki et al. 1997; Kenny et al. 1998; Wang et al. 2000) and Hirschsprung's disease (HD) (Yamataka et al. 1995; Horisawa et al. 1998). This investigation has shown clear age-dependent changes in the morphology and cell number (by proliferation) of ICCs during the postnatal developmental period. In this regard, the precursors of ICCs might be a potential target for the future disease treatment, either through in vivo and/or in vitro expansion of these cells and might be a feasible therapeutic strategy.

Acknowledgments This work was supported in parts by the national key basic research program of China (2007CB512401). We thank Dr. Thomas FitzGibbon for comments and discussion on earlier drafts of the manuscript, and also we are grateful to Wei Sun and Li-ting Wang (Central laboratory, Third Military Medical University) for their help with confocal laser scanning microscopy.

References

Beckett EA, Ro S, Bayguinov Y, Sanders KM, Ward SM (2007) Kit signaling is essential for development and maintenance of interstitial cells of Cajal and electrical rhythmicity in the embryonic gastrointestinal tract. Dev Dyn 236:60–72

Chang IY, Glasgow NJ, Takayama I, Horiguchi K, Sanders KM, Ward SM (2001) Loss of interstitial cells of Cajal and development of electrical dysfunction in murine small bowel obstruction. J Physiol 536:555–568

Faussone-Pellegrini MS, Matini P, Stach W (1996) Differentiation of enteric plexuses and interstitial cells of Cajal in the rat gut during pre- and postnatal life. Acta Anat (Basel) 155:113–125

Horiguchi K, Komuro T (2000) Ultrastructural observations of fibroblast-like cells forming gap junctions in the W/W(nu) mouse small intestine. J Auton Nerv Syst 80:142–147

Horisawa M, Watanabe Y, Torihashi S (1998) Distribution of c-Kit immunopositive cells in normal human colon and in Hirschsprung's disease. J Pediatr Surg 33:1209–1214

Huizinga JD, Thuneberg L, Kluppel M, Malysz J, Mikkelsen HB, Bernstein A (1995) W/kit gene required for interstitial cells of Cajal and for intestinal pacemaker activity. Nature 373:347–349

Huizinga JD, White EJ (2008) Progenitor cells of interstitial cells of Cajal: on the road to tissue repair. Gastroenterology 134:1252–1254

Isozaki K, Hirota S, Miyagawa J, Taniguchi M, Shinomura Y, Matsuzawa Y (1997) Deficiency of c-kit+ cells in patients with a myopathic form of chronic idiopathic intestinal pseudo-obstruction. Am J Gastroenterol 92:332–334

Kenny SE, Vanderwinden JM, Rintala RJ, Connell MG, Lloyd DA, Vanderhaegen JJ, De Laet MH (1998) Delayed maturation of the interstitial cells of Cajal: a new diagnosis for transient neonatal pseudoobstruction. Report of two cases. J Pediatr Surg 33:94–98

Kluppel M, Huizinga JD, Malysz J, Bernstein A (1998) Developmental origin and kit-dependent development of the interstitial cells of Cajal in the mammalian small intestine. Dev Dyn 211:60–71

Komuro T, Zhou DS (1996) Anti-c-kit protein immunoreactive cells corresponding to the interstitial cells of Cajal in the guinea-pig small intestine. J Auton Nerv Syst 61:169–174

Krishnamurthy S, Heng Y, Schuffler MD (1993) Chronic intestinal pseudo-obstruction in infants and children caused by diverse abnormalities of the myenteric plexus. Gastroenterology 104:1398–1408

Lecoin L, Gabella G, Le Douarin N (1996) Origin of the c-kit-positive interstitial cells in the avian bowel. Development 122:725–733

Lee JC, Thuneberg L, Berezin I, Huizinga JD (1999) Generation of slow waves in membrane potential is an intrinsic property of interstitial cells of Cajal. Am J Physiol 277:G409–G423

Liu LW, Thuneberg L, Huizinga JD (1998) Development of pacemaker activity and interstitial cells of Cajal in the neonatal mouse small intestine. Dev Dyn 213:271–282

Lorincz A, Redelman D, Horvath VJ, Bardsley MR, Chen H, Ordog T (2008) Progenitors of interstitial cells of Cajal in the postnatal murine stomach. Gastroenterology 134:1083–1093

Lu X, Zhao J, Gregersen H (2005) Small intestinal morphometric and biomechanical changes during physiological growth in rats. J Biomech 38:417–426

Mei F, Yu B, Ma H, Zhang HJ, Zhou DS (2006) Interstitial cells of Cajal could regenerate and restore their normal distribution after disrupted by intestinal transection and anastomosis in the adult guinea pigs. Virchows Arch 449:348–357

Nakahara M, Isozaki K, Vanderwinden JM, Shinomura Y, Kitamura Y, Hirota S, Matsuzawa Y (2002) Dose-dependent and time-limited proliferation of cultured murine interstitial cells of Cajal in response to stem cell factor. Life Sci 70:2367–2376

Ordog T, Ward SM, Sanders KM (1999) Interstitial cells of Cajal generate electrical slow waves in the murine stomach. J Physiol 518(Pt 1):257–269

Pucilowska JB, McNaughton KK, Mohapatra NK, Hoyt EC, Zimmermann EM, Sartor RB, Lund PK (2000) IGF-I and procollagen alpha1(I) are coexpressed in a subset of mesenchymal cells in active Crohn's disease. Am J Physiol Gastrointest Liver Physiol 279:G1307–G1322

Rumessen JJ, Thuneberg L (1991) Interstitial cells of Cajal in human small intestine: ultrastructural identification and organization between the main smooth muscle layers. Gastroenterology 100:1417–1431

Thomsen L, Robinson TL, Lee JC, Farraway LA, Hughes MJ, Andrews DW, Huizinga JD (1998) Interstitial cells of Cajal generate a rhythmic pacemaker current. Nat Med 4:848–851

Thomson AB, Keelan M (1986) The aging gut. Can J Physiol Pharmacol 64:30–38

Torihashi S, Nishi K, Tokutomi Y, Nishi T, Ward S, Sanders KM (1999) Blockade of kit signaling induces transdifferentiation of interstitial cells of Cajal to a smooth muscle phenotype. Gastroenterology 117:140–148

Torihashi S, Ward SM, Nishikawa S, Nishi K, Kobayashi S, Sanders KM (1995) c-kit-dependent development of interstitial cells and electrical activity in the murine gastrointestinal tract. Cell Tissue Res 280:97–111

Torihashi S, Ward SM, Sanders KM (1997) Development of c-kit-positive cells and the onset of electrical rhythmicity in murine small intestine. Gastroenterology 112:144–155

Vanderwinden JM, Liu H, De Laet MH, Vanderhaeghen JJ (1996a) Study of the interstitial cells of Cajal in infantile hypertrophic pyloric stenosis. Gastroenterology 111:279–288

Vanderwinden JM, Rumessen JJ, Liu H, Descamps D, De Laet MH, Vanderhaeghen JJ (1996b) Interstitial cells of Cajal in human colon and in Hirschsprung's disease. Gastroenterology 111:901–910

Wang ZQ, Watanabe Y, Toki A, Kohno S, Hasegawa S, Hamazaki M (2000) Involvement of endogenous nitric oxide and c-kit-expressing cells in chronic intestinal pseudo-obstruction. J Pediatr Surg 35:539–544

Ward SM, Harney SC, Bayguinov JR, McLaren GJ, Sanders KM (1997) Development of electrical rhythmicity in the murine gastrointestinal tract is specifically encoded in the tunica muscularis. J Physiol 505(Pt 1):241–258

Ward SM, McLaren GJ, Sanders KM (2006) Interstitial cells of Cajal in the deep muscular plexus mediate enteric motor neurotransmission in the mouse small intestine. J Physiol 573:147–159

Ward SM, Sanders KM (2001) Physiology and pathophysiology of the interstitial cell of Cajal: from bench to bedside. I: functional development and plasticity of interstitial cells of Cajal networks. Am J Physiol Gastrointest Liver Physiol 281:G602–G611

Wu JJ, Rothman TP, Gershon MD (2000) Development of the interstitial cell of Cajal: origin, kit dependence and neuronal and nonneuronal sources of kit ligand. J Neurosci Res 59:384–401

Yamataka A, Kato Y, Tibboel D, Murata Y, Sueyoshi N, Fujimoto T, Nishiye H, Miyano T (1995) A lack of intestinal pacemaker (c-kit) in aganglionic bowel of patients with Hirschsprung's disease. J Pediatr Surg 30:441–444

Yanagida H, Yanase H, Sanders KM, Ward SM (2004) Intestinal surgical resection disrupts electrical rhythmicity, neural responses, and interstitial cell networks. Gastroenterology 127:1748–1759

Young HM (1999) Embryological origin of interstitial cells of Cajal. Microsc Res Tech 47:303–308

Young HM, Ciampoli D, Southwell BR, Newgreen DF (1996) Origin of interstitial cells of Cajal in the mouse intestine. Dev Biol 180:97–107

Zhou DS, Komuro T (1992) Interstitial cells associated with the deep muscular plexus of the guinea-pig small intestine, with special reference to the interstitial cells of Cajal. Cell Tissue Res 268:205–216